

2D-3D Feature Extraction and Registration of real World Scenes

AUTHORS

Yahya Alshawabkeh / Norbert Haala /
Dieter Fritsch

Abstract

In this paper we present an efficient edge detection algorithm for the extraction of linear features in both range and intensity image data. The purpose is to simplify the dense datasets and to provide stable features of interest, which are used to recover the positions of the 2D cameras with respect to the geometric model for tasks such as texture mapping. In our algorithm the required features of interest are extracted by an analysis of the mean curvature values. As it will be demonstrated, the algorithm features computational efficiency, high accuracy in the localization of the edge points, easy implementation, and robustness against noise. The generality and robustness of the algorithm is illustrated during processing of complex cultural heritage scenes.

Zusammenfassung

2D-3D Objekterkennung und Registrierung von Bildern und Punktwolken

Der Beitrag führt einen neuen, effizienten Kantenfindungsalgorithmus für Bilder und Punktwolken ein. Zum einen werden dichte Punktwolken vereinfacht und Objektfeatures identifiziert, die für die Rekonstruktion der äußeren Orientierung eingesetzt werden und ein anschließendes Texturmapping ermöglichen. Die Kantenelemente werden über mittlere Krümmungsmaße extrahiert. Der Algorithmus zeichnet sich durch geometrische Effizienz, hohe Genauigkeit der Kantenpunkte, leichte Implementierung und Robustheit gegenüber Rauschen aus. Seine allgemeine Anwendung und Robustheit wird durch die Anwendung auf komplexe Datensätze von Baudenkmalern nachgewiesen.

1. Introduction

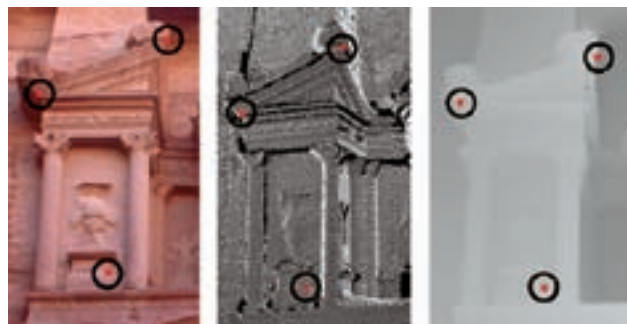
Terrestrial laser scanning has become a standard tool for 3D data collection to generate high quality 3D models of cultural heritage sites and historical buildings [Boehler and Marbs, 2002]. Based on the run-time of reflected light pulses these systems allow for the fast and reliable measurement of millions of 3D points allowing for a very effective and dense measurement of the surface geometry. In addition to the geometric data collection, texture mapping is particular important in the area of cultural heritage in order to allow a complete documentation of the respective sites. For this reason, some commercial 3D systems provide model-registered color texture by the simultaneous collection of RGB values of each LIDAR point. For this purpose a camera is directly integrated in the system. However, the ideal conditions for taking images may not coincide with those for laser scanning [El-Hakim et al, 2002]. For this reason, these images frequently will not be sufficient for high quality texturing as it is usually desired for documentation and visualisation purposes. In addition, laser scanning is frequently required from many viewpoints to capture complex object structures, which results in a relatively time consuming process. For outdoor applications these large time differences will result in varying light conditions and changing shadows, therefore the captured images will feature different radiometric properties. Such problems will considerably disturb the visual appearance of the resulting textured model. In order to allow for an image coll-

ection at optimal position and time for texturing it is advantageous to acquire geometry and texture by two independent processes. This is especially true for the high requirements, which have to be met for the realistic documentation of heritage sites.

To allow for a combined evaluation of the collected range and image data sets, co-registration or alignment has to be performed as the first processing step. For this purpose corresponding elements are required. However, the automatic extraction and matching of suitable primitives such as points, corners, and lines is extremely difficult especially in complex scenes [Ferencz, 2001]. An alternative way is the use of artificial targets like spheres or signals, which can be detected and identified more easily in both laser range data and intensity images [Yu et al, 2000]. However, this requires additional effort during data collection and management. Additionally, time-consuming high-resolution scanning is required to accurately measure the position of the target center. Moreover, these artificial objects may occlude important parts of the intensity images, which are required for texture mapping [Lensch et al, 2000]. Alternatively, user supplied corresponding primitives like 3D points or lines and their 2D projections on the image plane can be used. Many solutions have been developed for pose estimation based on such 2D-3D correspondences.

A number of traditional photogrammetric approaches use point matches, which allow for direct solutions based on three, four or six corresponding points

Fig. 1: Limited perception in finding the corresponding points in point clouds and range image.



Abbildungen: Alshawabkeh, Haala, Fritsch

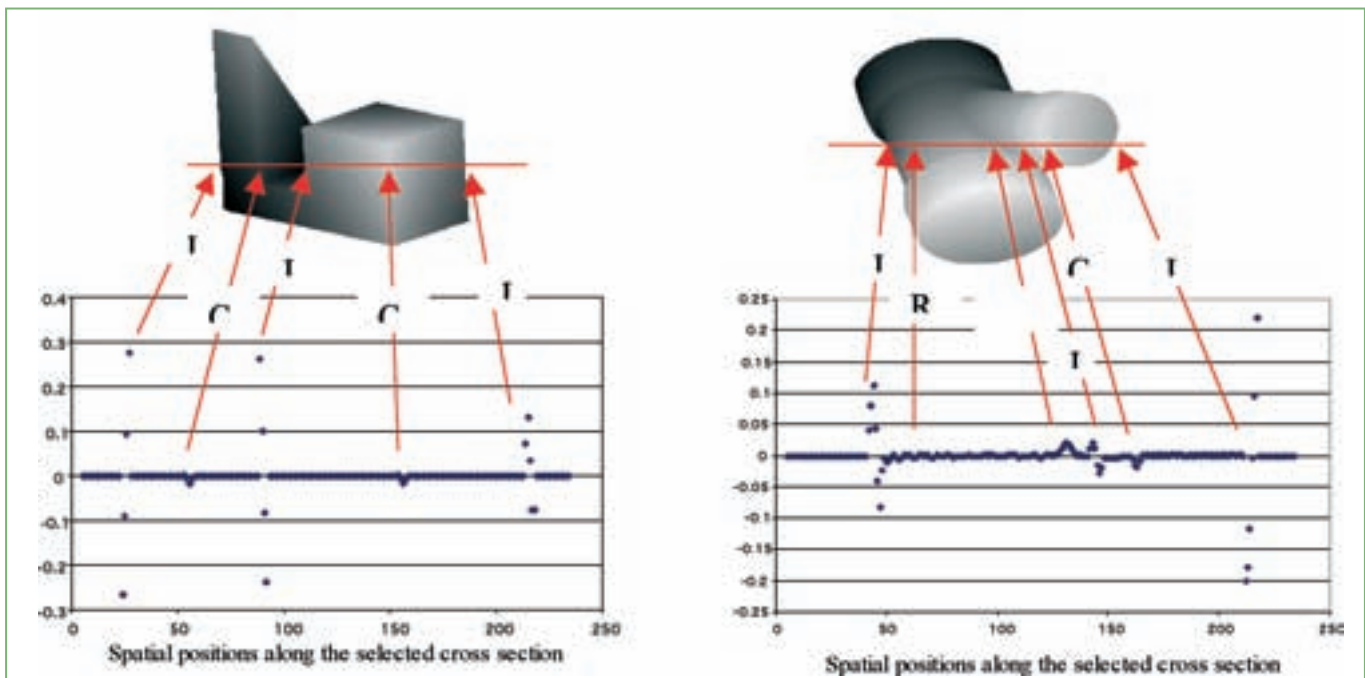


Fig. 2: Spatial distribution of the mean curvature values for block and wye range image.

[Haralick et al, 1994]. However, the perception of such point structures is limited within range data and can result in an accuracy of manual measurement which is not appropriate for registration [Liu & Sotom, 2005]. This is demonstrated exemplarily for a cultural heritage application in Figure 1. While point features can be identified well in the image (left), an exact measurement within the corresponding 3D point cloud (middle) or the range image (right) from laser scanning is difficult. For this reason, the use of linear features is advantageous. From a practical point of view, line detection is more accurate and more reliable than points, line matching is also more robust than point matching with respect to partial occlusions [Christy & Horaud, 1999]. Those features can also help to increase the reliability of the adjustment during spatial resection. In addition to the fact that linear features frequently occur within images of man-made environments, it is easier to automatically extract such edge structures compared to a measurement of distinct points [Horaud et al, 1997, Lee & Habib, 2002]. In order to automatically provide stable features of interest, efficient segmentation algorithms are required. Most of these segmentation algorithms are based on range images instead of unordered 3D point clouds [Yu & Ferencz, 2001]. For such 2.5D raster grids

neighborhood relations are available implicitly and tools from image processing can be adopted. Thus, the implementation of segmentation algorithms is simplified considerably.

Within the paper an efficient algorithm for the detection of edge structures in both range and intensity images is presented. By these means, stable features of interest are provided. They allow for an accurate alignment of the range and image data which is required for the generation of high quality and photo-realistic 3D models. Within the paper, the presented approach is demonstrated in the framework of a project aiming at the generation of a 3D virtual model of the Al-Khasneh, a well-known monument in Petra, Jordan.

2. Related Work

Algorithms developed for the segmentation of intensity images have been discussed extensively in the literature. Well-known examples for the real-time segmentation of intensity images are [Palmer et al, 1996; Canny, 1986]. In the other hand, ready-made solutions for range image segmentation are not available to a comparable extent [Gächter, 2005]. Similar to image processing, existing approaches can be categorized in region-based and edge-based techniques. Region-based approaches group range pixels into connected re-

gions using some homogeneity measure. For each region, an approximating surface model is computed. Different range image segmentation algorithms based on region growing were analyzed systematically in [Hoover et al, 1996]. There the authors also conclude that range image segmentation is still not really a solved problem even for simple industrial scenes containing polyhedral objects. More recent publications are e.g. given in [Marchall et al, 2001; Melkemi & Sapidis, 2002]. Range data is usually well suited for the extraction of smooth or planar surface patches, while the accuracy of directly extracted edges is limited. This results from the fact that range measurement is usually noisy at such discontinuities mainly due to multipath effects. For this reason only a few segmentation algorithms use edge-based techniques [Sze et al, 1998; Vitulano & Maniscalco, 2004; Katsoulas & Werber, 2004]. Most of these approaches are again focused on simple polyhedral objects and are limited to the detection of specific structures such as straight lines or circles.

While in the past range data collection was mainly applied for industrial scenes captured at close distances, nowadays long-range laser scanners are available for many users. By these means detailed data sets of complex outdoor scenes are collected, which pose much more se- ►

rious challenges for range image analysis than the traditional polyhedral world. The difficulties result from the fact that range data of natural scenes are relatively noisy. These measurement errors affect the approximation of the surfaces during segmentation. In addition, the natural scenes are complex since lots of individual objects or irregular surfaces occur. For segmentation of this type of data [Sappa et al, 2001] propose a two step approach. The first step generates a binary edge map based on a scan line approximation technique as e.g. proposed by [Jiang & Bunke, 1999]. The second step aims on contour extraction by a weighted graph. A minimum spanning tree (MST) is computed to obtain the shortest path, which links all the edge points. One of the main drawbacks of this algorithm is the fact that during the MST filtering many edges are eliminated. Recently [Han et al, 2004] presented a stochastic jump-diffusion algorithm for the segmentation of range images in a Bayesian framework. The algorithm can be used for processing of complex real-world scenes. Although it is considered as the most advanced algorithm for complex scene segmentation, some drawbacks such as computational complexity and the large number of required parameters are still mentioned. In addition, suitable a priori assumptions are required.

Some existing algorithms are limited to high quality range images and will fail in the presence of noise. Others are complicated and have a large numbers of parameters while generic and efficient edge detectors for range images are still missing. This was our motivation for the development of an edge detection algorithm for range images, which is presented in the following.

3. ALGORITHM DESCRIPTION

3.1 Methodology

The approach is based on the analysis of classical differential geometry of 3D surfaces. In our algorithm, the distinguished points, which will comprise the edges within the range image, are extracted by the spatial analysis of the numerical description of the mean curvature values. For this purpose, the surface is locally approximated by an analytic representation. The different properties of the patch at the respective points of interest are then calculated analytically. In order to benefit

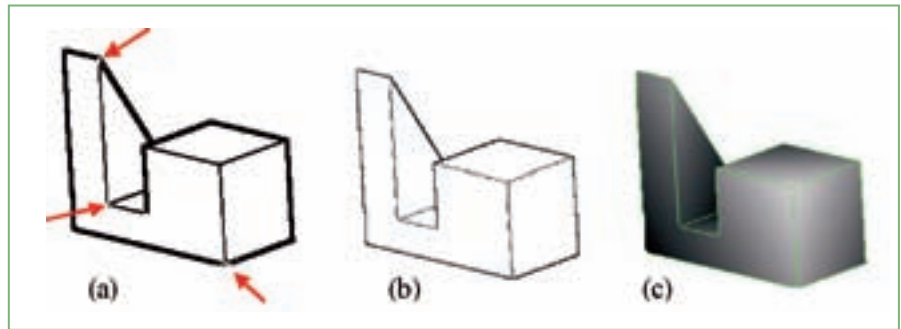


Fig. 3: a) Depth and discontinuities detection using mask size 5, the red arrows show the missing parts in the junction and the corners of the object. b) Handling the junction problems using different scale threshold parameters. c) Segmentation result after thinning process to yield one pixel wide edge.

from the behaviour of the mean curvature at edges, the algorithm detects local maxima or zero crossings in the range image. Further processing steps like a multi-scale edge detection and a subsequent skeletonization are used to increase the reliability and accuracy during the edge detection and localization.

3.2 Mathematical Properties of Mean Curvature Values

In general, successful segmentation requires an appropriate surface description. This description should be rich, so that matches of similar elements can be detected, stable so that local changes do not radically alter the descriptions, and it should have a local support so that the visible objects can be easily identified. These characteristics are provided by the mathematical properties of the mean curvature, which is closely related to the first variation of a surface area. Unlike the Gaussian curvature, the mean curvature depends on the embedding, for instance, a cylinder and a plane are locally isometric but the mean curvature of a plane is zero while that for a cylinder is non-zero. Mean curvature is invariant to arbitrary rotations and translation of surface, which is important for surface shape characterization. Since mean curva-

ture is the average of the principal curvatures, it is slightly less sensitive to noise during numerical computations. Due to these characteristics, mean curvature values can provide stable and useful measures for detecting surface features in range and intensity images.

Several techniques are known for the efficient estimation of the mean curvature. The frequently applied analytical methods fit a surface in a local neighbourhood of the point of interest. This surface approximation is then used to compute the partial derivatives needed to calculate the curvature values. As an example [Besl & Jain, 1988] proposed an analytical technique for estimating the mean and Gaussian curvature. The advantage of this approach is its flexibility to estimate the curvature values at multiple scales, and the efficient computation of the values by optimized convolution operations. For these reasons, the estimation of the mean curvature values in our algorithm is also based on a modification of this approach. It can be summarized as follows: For a given odd $N \times N$ window, each data point is associated with a position (u, v) from the set $U \times U$ where

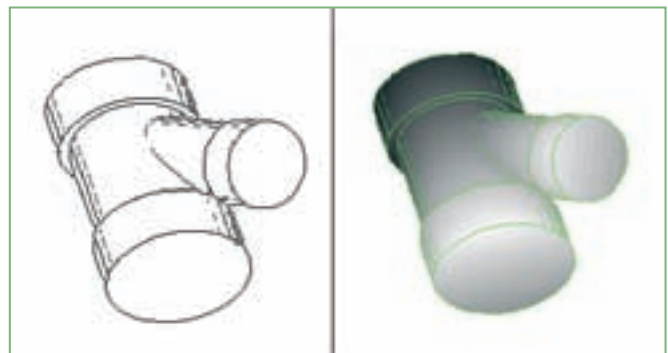


Fig. 4: Segmentation results for wye image.

$$U = \{-(N-1)/2, \dots, -1, 0, 1, \dots, (N-1)/2\}$$

The local biquadratic surface fitting capability is provided using the following discrete orthogonal polynomials:

$$\begin{aligned} \mathcal{O}_0(u) &= 1, \mathcal{O}_1(u) = u, \mathcal{O}_2(u) = \\ &= (u^2 - M(M+1)/3); M = (N-1)/2 \end{aligned}$$

To estimate the first and second partial derivatives, an orthogonal set of $d_i(u)$ functions using the normalized versions of the orthogonal polynomials $\mathcal{O}_i(u)$ is used:

$$\vec{d}_i(u) = \frac{\mathcal{O}_i(u)}{P_i(M)}, P_0(M) = N, P_1(M) = \frac{2}{3}M^3 + M^2 + \frac{1}{3}M$$

$$P_2(M) = \frac{8}{45}M^5 + \frac{4}{9}M^4 + \frac{2}{9}M^2 - \frac{1}{15}M$$

Since the discrete orthogonal quadratic polynomials over the 2D window are separable in u and v , partial derivative estimates can be computed using separable convolution operators. These derivatives estimates can then be plugged into the equation for mean curvature. The equally weighted least squares derivative estimation window operators are then given by:

$$[D_u] = \vec{d}_0 \vec{d}_1^T, [D_v] = \vec{d}_1 \vec{d}_0^T, [D_{uu}] = \vec{d}_0 \vec{d}_2^T,$$

$$[D_{vv}] = \vec{d}_2 \vec{d}_0^T, [D_{uv}] = \vec{d}_1 \vec{d}_1^T$$

$\tilde{g}(i,j)$ represents the noisy, quantized discretely sampled version of a piecewise-smooth graph surface. Then the partial derivative estimate images are computed via appropriate 2D image convolutions.

$$\begin{aligned} \tilde{g}_u(i,j) &= D_u \otimes \tilde{g}(i,j), \tilde{g}_v(i,j) = D_v \otimes \tilde{g}(i,j), \\ \tilde{g}_{uu}(i,j) &= D_{uu} \otimes \tilde{g}(i,j), \tilde{g}_{uv}(i,j) = D_{uv} \otimes \tilde{g}(i,j), \\ \tilde{g}_{vv}(i,j) &= D_{vv} \otimes \tilde{g}(i,j), \end{aligned}$$

The mean curvature is then computed using the partial derivatives estimates as the following:

$$\begin{aligned} H(i,j) &= \{(1 + \tilde{g}_v^2(i,j))\tilde{g}_{uu}(i,j) + (1 + \tilde{g}_u^2(i,j)) \\ &\tilde{g}_{vv}(i,j) - 2\tilde{g}_u(i,j)\tilde{g}_v(i,j)\tilde{g}_{uv}(i,j)\} / \\ &2(\sqrt{1 + \tilde{g}_u^2(i,j) + \tilde{g}_v^2(i,j)})^3 \end{aligned}$$

3.3 Mean Curvature Spatial Analysis

The behaviour of the mean curvature for specific object properties can be demon-



Fig. 5: Curve block segmentation using different thresholds to detect step edges (red) and crease edges (blue).

strated well by the filter results for synthetic range images. Thus the mean curvature was computed for range images of a block and a wye, which are depicted in Figure 1. The curvature values were then extracted at the horizontal profile represented by the line overlaid to the respective range image. From the analysis of these curvature values as they are depicted in the bottom of Figure 1 one can conclude the following:

a) For jump edge boundaries (J) where surface depths are discontinuous, the mean curvature exhibits a zero crossing. Two distinct peaks of opposite algebraic sign are clearly visible in the profile of computed curvature values.

b) For crease edges (C) at discontinuities in the surface normal direction, the curvature response is a smooth peak. Concave (Cv) and convex (Cx) edges can be discriminated by the different algebraic sign of the curvature values. The exact position of a convex crease edge is defined by the maximum curvature value, while the concave crease edge is given at a minimum.

c) At ridges (R) the mean curvature also indicates a change in the orientation of the surface normal, however, the response is smaller compared to crease edges.

d) Compared to crease edges, the values of the mean curvature are larger at jump edges. Their value mainly depends on the magnitude of the depth discontinuity.

e) For jump edges, the exact position is defined at a zero crossing between two peaks of the mean curvatures, whereas for both crease and ridge edges the true edge is given by the maximum and minimum value of the peaks.

After computation of the mean curvature values $H(x,y)$ a pixel represents an edge location $\{(x,y): E(x,y)=1\}$ if the value of the gradient exceeds some threshold. Thus:

$$E(x,y) = \begin{cases} 1 & \text{if } \|H\| > T \text{ for some threshold } T \\ 0 & \text{otherwise} \end{cases}$$

In order to locate the position of crease, ridge and step edges, zero crossings as well as smooth peak values are searched within the computed mean curvature values during the edge detection process.

3.4 Multi-Scale Approach

Of course the effectiveness of edge detection is related to the signal-noise ratio of the data. Small-scale operators can detect fine details within range images but are sensitive against noise. In contrast, the mean curvature can be estimated more reliable using larger mask sizes of the filter operator. However, in this configuration a number of edges can not be detected. This is especially a problem for closely neighbored edges e.g. at intersections. This is clearly visible in Figure 3a, where missing edge pixels are marked by the red arrows.

Since no single edge operator performs optimal for all scales, a compromise between edge localization and noise sensitivity is aspired by a multi-scale approach. By these means the missing edges are recovered correctly, as it is visible in Figure 3b. Such multi-scale approaches apply different sizes of edge operators on an image, thus different descriptions are generated where new extreme points may appear. Since the width of an edge will expand as the scale increases, a thinning process is performed to yield one pixel wide edges. One criterion during evaluation of edge strength is that the extracted edges should be continuous and provide a connected thin line in the binary image. The result of this skeletonization is depicted in Figure 3c. Figure 4 depicts an additional result of edge extraction and skeletonization for the wye data set. The figure shows that the algorithm has the ability to detect the ridges lines, which are correspond to local extrema of the mean curvature values.

4. Algorithm Characteristics

Good edge detection requires an operator, which is designed to fit the nature of a specific image. Additionally, some other characteristics of the proposed edge detector related to the nature and properties of the mean curvature will be discussed in the following.

4.1 Crease-step edge Classification

As it was already discussed in section 3, the value of the mean curvature is smaller for crease edges than for jump edges. Based on this definition, the edge types of an object can be classified easily by applying different threshold values. Low threshold values are used to detect the

small peaks of crease edges while larger values can be used for step edge detection.

The example of a curve block in Figure 5 demonstrates this ability of our algorithm to reliably characterize these edge types.

4.2 Real Scene Segmentation

The main challenge for most of segmentation algorithms is the robustness against noise. Thus, a number of edge detection techniques apply a smoothing process before the extraction of range changes. However, this smoothing limits the accuracy of the edge localization. In general, mean curvature is slightly less sensitive to noise in numerical computation since it is the average of the principal curvatures.

In order to examine the robustness of our approach against noise, and to demonstrate its ability to deal with a variety of object surfaces, a test with a complex real world scene was applied.

Figure 6a displays two range data sets for the 3D model of Al-Khasneh (Petra treasury), which were collected by a Mensi GS100 laser scanner. The processing is based on range images,

which maintain the original topology of a laser scan. Thus, compared to the processing of unordered 3D point clouds the segmentation can be implemented more easily. The top row of Figure 6 depicts data from the outer façade of Al-Kahsneh, while the bottom row shows data collected for one of the interior rooms. Since such data are usually contaminated by noise, a large mask size of 11 pixel was used to allow for a reliable edge detection. Figure 6b shows the binary edge maps as they are generated using the proposed segmentation process. As it is visible, most of the main features are detected. Since a large mask size was used, the edges are rather blurred. For this reason, the edges are then sketolozed by the thinning process. Figure 6c depicts the results of this process overlaid to the corresponding range image. As it is depicted in Figure 6d the technique described above for range image processing can also be used to segment intensity images.

5. Conclusion

Frequently a combination of terrestrial LIDAR and image data is applied during 3D reconstruction of complex terrestrial

scenes in the context of cultural heritage applications. A successful integration of both data sources will support tasks like surface reconstruction and will facilitate subsequent processing activities such as the generation of 3D textured models. The combination of the different data sets requires an exact co-registration, which has to be solved by a 2D-3D pose estimation algorithm. The most common methods for solving such registration problems between two datasets are based on the identification of corresponding points. Such methods are not applicable when dealing with LIDAR surfaces, since they correspond to laser footprints with limited scanning resolution rather than distinct points that could be identified in the imagery. Additionally, in the application of point clouds and range images, the perception of objects structure is limited and not very appropriate for registration.

Hence, our goal is to reach a very precise and reliable co-registration of data sets. Linear features possess higher semantic information, which is desirable for this purpose. In this case, the correspondence problem between the image and object space can be solved easier.

Fig. 6: a) Range images for 3D model of Al-Khasneh. b) Binary edge image produced using the proposed segmentation algorithm. c) Segmentation results after thinning process projected in the corresponding range image. d) Segmentation results of colored images using the proposed algorithm, the red arrows show some selected edges used for registration of 2D-3D data sets.



In our approach for automatic texture mapping [Alshawabkeh & Haala, 2005], we have used the methodology for extracting the linear features from range and intensity image using the proposed segmentation algorithm. Then, aligning of the extracted edges is realized using an algorithm developed by [Klinec and Fritsch, 2003]. Figure 6c and Figure 6d exemplarily show some manually selected edges (lines) used to register both colour and range images for Petra treasury (Al-Khasneh).

The quality of the registration process, which aligns the laser scanner data with the imagery, is a crucial factor for the combined processing. Since the accuracy of the transformation depends on the reliable extraction of primitives from the range and intensity images, efficient edge detection as it is feasible by the proposed algorithm is an important task for a combined evaluation of this type of data. ■

AUTHORS

Yahya Alshawabkeh / Norbert Haala / Dieter Fritsch

Institute for Photogrammetry (ifp),
Universitaet Stuttgart, Germany
Geschwister-Scholl-Strasse 24D,
D-70174 Stuttgart

yahya.alshawabkeh@ifp.uni-stuttgart.de
norbert.haala@ifp.uni-stuttgart.de
dieter.fritsch@ifp.uni-stuttgart.de

References

- Alshawabkeh, Y. & Haala N. [2005], Automatic Multi-Image Photo Texturing of Complex 3D Scenes. CIPA IAPRS Vol. 34-5/C34, pp. 68-73.
- Besl, P. & Jain, R. [1988], Segmentation Through Variable-Order Surface Fitting. IEEE Transactions on Pattern Analysis and Machine Intelligence, 9(2): 167-192.
- Boehler, W., Marbs, A., 2002. 3D scanning instruments. ISPRS/CIPA International Workshop on Scanning for Cultural Heritage Recording, Corfu, Greece, pp.9-12.
- Bruni, V., Vitulano, D. & Maniscalco, U. [2004], Fast Segmentation and Modeling of Range Data Via Steerable Pyramid and Superquadrics. The 12-th International Conference in Central Europe on Computer Graphics, Visualization and Computer Vision'2004, WSCG 2004, University of West Bohemia, Czech Republic.
- Canny, J. [1986], A Computational Approach to Edge Detection, IEEE Transactions on Pattern Analysis and Machine Intelligence, Vol. 8, No. 6, Nov.
- Christy, S. & Horaud, R. [1996], Iterative Pose Computation from Line Correspondences. Computer Vision and Image Understanding Vol. 73, No. 1, January, pp. 137-144.
- Djebali, M., Melkemi, M. & Sapidis, N. [2002], „Range-Image Segmentation and Model Reconstruction Based on a Fit-and-Merge Strategy“, ACM Symposium on Solid Modeling and Applications, pp.127-138.
- El-Hakim, S., Beraldin, A. & Picard, M. [2002], Detailed 3D reconstruction of monuments using multiple techniques. ISPRS /CIPA .Corfu, Greece, pp.58-64.
- Ferencz, A. [2001], Texture Mapping Range Images. Masters Thesis, Computer Science Division, EECS, UC Berkeley.
- Gächter, S. [2005], Results on range image segmentation for service robots. Technical Report. Switzerland.
- Han, F., Tu, Z. & Zhu, S. [2004], Range image segmentation by an efficient jump-diffusion method. In IEEE Trans. On Pattern Analysis and Machine Intelligence. Vol.26/9. pp.1138-1153.
- Haralick, R., Lee, C., Ottenberg, K. & Nolle, M. [1994], Review and analysis of solutions of the 3-point perspective pose estimation problem. IJCV 13(3), pp. 331-356.
- Horaud, R., Dornaika, F., Lamiroy, B. & Christy, S. [1997], "Object pose: The link between weak perspective, paraperspective, and full perspective," Int. J. Comput. Vision, vol. 22, no. 2, pp. 173-189.
- Hoover, A., Jean-Baptiste, G. & Jiang, X. [1996], An Experimental Comparison of Range Image Segmentation Algorithms. IEEE Transactions on Pattern Analysis and Machine Intelligence, 18(7): p. 673-689.
- Jiang, X. & Bunke, H. [1999], Edge detection in range images based on scan line approximation. Computer Vision and Image Understanding: CVIU, 73(2): 183-199.
- Katsoulas, D. & Werber, A. [2004], Edge Detection in Range Images of Piled Box-like Objects. 17th International Conference on Pattern Recognition (ICPR 2004), 4-Volume Set, Cambridge, UK. IEEE Computer Society, ISBN 0-7695-2128-2. pp 80-84.
- Klinec, D. & Fritsch, D. [2003], Towards pedestrian navigation and orientation. Proceedings of the 7th South East Asian Survey Congress: SEASC'03, Hong Kong, November 3-7.
- Lee, Y. & Habib, A. [2002], Pose Estimation of Line Cameras Using Linear Features, ISPRS Symposium of PCV'02 Photogrammetric Computer Vision, Graz, Austria.
- Lensch, H., Heidrich, W. & Seidel, H. [2000], Automated texture registration and stitching for real world models. In Proceedings of Pacific Graphics 2000, pages 317-326.
- Liu, L. & Stamos, S. [2005], Automatic 3D to 2D registration for the photorealistic rendering of urban scenes. Computer Vision and Pattern Recognition. IEEE Computer Society.
- Marshall, D., Lukacs, G. & Martin, R. [2001], Robust segmentation of primitives from range data in the presence of geometric degeneracy; IEEE Trans. Pattern Analysis and Machine Intelligence 23(3), 304-314.
- Ohio State University range Image Collection, <http://sampl.ece.ohio-state.edu/data/>.
- Palmer, P., Dabis, H. & Kittler, J. [1996] A performance measure for boundary detection algorithms. CVGIP: Image Understanding, 63(3): 476-494.
- Sappa, A. & Devy, M. [2001], "Fast Range Image Segmentation by an Edge Detection Strategy," Proc. IEEE Conf. 3D Digital Imaging and Modeling, pp. 292-299.
- Sze, C., Liao, H., Hung, H., Fan, K. & Hsieh, J. [1998], "Multiscale edge detection on range images via normal changes," IEEE Transition. Circuits System. II, vol. 45, pp. 1087-1092.
- Yu, Y., & Ferencz, A., [2001] Extracting Objects from Range and Radiance Images. IEEE Transactions on Visualization and Computer Graphics, Vol 7, No.4.
- Yu, Y., Ferencz, A. & Malik, J. [2000] Compressing Texture Maps for Large Real Environments. SIGGRAPH'2000.